Dielectric and Tensile Behavior of Nanoclay Reinforced Polyetherimide Nanocomposites

Mayank Dwivedi,[1,2] Alok Dixit,[3] Sarfaraz Alam,[3] Anup K. Ghosh[1]

[1]*Centre for Polymer Science and Engineering, Indian Institute of Technology Delhi, Hauz Khas, New Delhi 110 016, India*
[2]*Defence Research and Development Organisation, DRDO Bhawan, Rajaji Marg, New Delhi 110 105, India*
[3]*Defence Materials and Stores Research & Development Establishment, DMSRDE PO, Kanpur 208 004, India*

Received 2 June 2010; accepted 25 January 2011
DOI 10.1002/app.34196
Published online 20 May 2011 in Wiley Online Library (wileyonlinelibrary.com).

ABSTRACT: Polyetherimide (PEI)/organoclay (Cloisite 30B) nanocomposite and PEI/pristine nanoclay (K10) nanocomposite were made by solution casting process. Nanoclay content of 0.5, 1.0, 2.0, and 3.0% (by weight) was reinforced in PEI. The dielectric properties (dielectric constant, loss tangent, and electromagnetic transmission/reflection losses) of PEI/Cloisite 30B were observed lower than PEI/K10 in X band frequency (8 to 12 GHz). Mixed morphology in terms of intercalation and exfoliation was evident in wide-angle X-ray diffraction (WAXD) analysis and transmission electron micrographs (TEM) of PEI/Cloisite 30B. Whereas, in PEI/K10, immiscibility, segregation, and phase separation of K10 were observed in WAXD analysis and scanning electron micrographs (SEM). Tensile properties (tensile strength, modulus, and elongation at break) of PEI/Cloisite 30B were superior to PEI/K10. Reinforcement with 1%, by weight, of Cloisite 30B in PEI resulted in the optimum properties, among all the compositions. © 2011 Wiley Periodicals, Inc. J Appl Polym Sci 122: 1040–1046, 2011

Key words: dielectric properties; mechanical properties; morphology; nanocomposites; organoclay

INTRODUCTION

Radar transparent materials (RTMs) are used in the nose cones of aircrafts for communication, protective covers for AWACS (Airborne warning and control systems), radomes (*ra*dar + *dome*) for missiles, protective covers for satcom (*sat*ellite + *com*munication) antenna, etc. For such applications, RTMs should be mechanically strong to survive operational loads as well as transparent to the electromagnetic (EM) wave. Transmission loss and reflection loss are the important parameters to decide on EM transparency of RTMs. Among polymeric nanocomposites (PNCs), nanoclay reinforced PNCs are good candidate as RTMs. Nanoclays have unique layered structure, intercalation chemistry, environmental stability, good processability, easy availability, cost effectiveness and above all low values of dielectric constant and loss tangent. The intercalation and exfoliation of nanoclay play an important role in the properties of nanoclay reinforced PNCs. Tsai et al.[1] have reported that well dispersed platelets of organoclay in polymer matrix can significantly enhance the mechanical properties of PNCs. Shabeer et al.[2] and Tsay et al.[3] have reported a drastic increase in tensile strength and modulus of nanoclay reinforced PNCs. Dwivedi et al.[4,5] have reported that dispersion of organoclay in the matrix has an important role in the properties of PNCs.

The use of high-temperature polymer matrix makes these PNCs suitable for high performance applications. Among high temperature polymers, polyetherimide (PEI) has good mechanical, thermal, and electrical properties as reported by Zebouchi et al.[6] Chen et al.[7] have reported that PEI has low dielectric constant, therefore, it is a good choice for application in electronics. The dielectric response originates from dipole orientation and exfoliation and intercalation of nanoclay have a role in the orientation of dipoles in PNCs. Wang et al.[8,9] have reported that the reinforcement of nanoclay in polystyrene has marginally reduced the dielectric constant and loss tangent of PNC. Whereas, Kashani et al.[10] have reported that dielectric constant of silicone rubber increased with the reinforcement of organoclay. Zhang et al.[11] have studied the dielectric properties of polyimide (PI)/nanoclay composites and reported that there was an increase in dielectric constant of PI/organoclay nanocomposite at 1% (by wt.) reinforcement of organoclay but, with further increase in the quantity of organoclay in PI, there

Correspondence to: M. Dwivedi (mayank.iitdelhi@gmail.com).

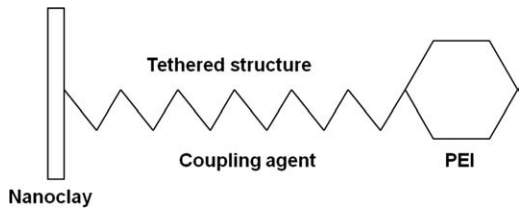

Figure 1 Schematic representation of tethered structure between nanoclay and PEI.

was a slight decrease in dielectric constant. According to McBrearty et al.,[12] dielectric properties were more uniform in PNCs with exfoliated organoclays than with intercalated organoclays.

Dhibar et al.[13] and Farzana et al.[14] have reported melt blending, solution casting and *in situ* polymerization as the methods of preparing PNCs. The commercially available polymers can only be processed either by melt blending or solution casting, for making PNCs. Mechanical mixing and sonication, for fabrication of PNCs, have been reported by Maroulas et al.[15] The fabrication of PEI films by solvent evaporation method has also been reported by Huang et al.[16] According to Morgan et al.,[17] organically treated nanoclay improves the miscibility of nanoclay in the polymer solution. Weiping et al.[18] have reported that an increase in basal spacing of nanoclay was observed when it was dispersed in solvent and polymer solution. The surface of Cloisite 30B specifically has methyl tallow bis-2-hydroxyethyl ammonium and this makes the surface of nanoclay hydrophobic. The hydrophobicity Cloisite 30B surface promotes van der Waals interaction, polar interaction, etc. with PEI and lead to formation of tethered structure between PEI and Cloisite 30B as shown schematically in Figure 1.

The presence of bis-2-hydroxy ethyl group, on the surface of Cloisite 30B, has the potential to react with —CONR— group of PEI to form hydrogen bond.

The aim of this work was to carry out the comparative study and analyze dielectric properties, tensile properties, and transparency to EM wave of PEI, PEI/Cloisite 30B, and PEI/K10 nanocomposites along with the morphology.

EXPERIMENTAL

PEI (Grade: Ultem 1000) was chosen as matrix and it was supplied by GE Plastics, USA. Organoclay (Cloisite 30B) was supplied by Southern Clay Products, USA and pristine nanoclay (K10) was supplied by Lancaster, UK. Cloisite 30B and K10 were used separately to compare their effects in PNC. N,N′-Dimethyl acetamide (DMAc) was chosen as the solvent for PEI. It was supplied by RANKEM Chemicals, India. The PEI/nanoclay nanocomposite films were prepared by solution casting method. In this method, PEI was dissolved in DMAc to make PEI/DMAc solution. Nanoclay was sonicated in DMAc, then mixed in PEI/DMAc solution and casted on mold. The homogenous solution of DMAc/PEI/nanoclay was casted on a mold which was accurately leveled by the help of spirit level so that the maximum possible flatness of the casted film was ensured. The PNC film was obtained by evaporating the DMAc. The temperature was increased gradually up to 190°C.[5] The rate of the heating was 15°C/min. The casted film was allowed to cool naturally to room temperature before demolding. The thickness of PEI and PNC films were 200 μm ± 10 μm and diameter was 200 mm.

The composition of casted films of PEI and PNCs are given in Table I.

PEI and PNC films were tested for tensile strength, modulus, and elongation at break as per ASTM 882 on a Universal Testing Machine (Model: 945 a, Make: Star Testing System, India). The crosshead speed was kept 5 mm per minute. Dielectric constant of Cloisite 30B and K10, were measured at X band frequency region (8.2–12.4 GHz) on a Dielectric Probe Kit (Model: Agilent 85070E, Frequency range: 200 MHz to 50 GHz, Make: Agilent Technologies) with high temperature probe. The error margin with high temperature probe was less than 2%. For this measurement, a pallet of 20-mm diameter and 20-mm thickness was made in a hydraulic machine. This test set up was calibrated using standard short and distilled water (at 25°C). The results were verified for air.

PEI and PNC films were tested for dielectric constant and transmission loss at X band frequency using Vector Network Analyzer (Model: PNA E 8364B, Make: Agilent Technologies, USA) and X band waveguide setup. Material Measurement Software (Model: 85071E, Make: Agilent Technologies) was used for calibration and measurement. Full two port calibration was carried out using TRL

TABLE I
Compositions of PEI/Nanoclay PNCs

S. No.	Sample No.	Weight % of PEI	Weight % of nanoclay
1	PEI	100	0
2	PN1	99.5	0.5 (K10)
3	PN2	99.0	1.0 (K10)
4	PN3	98.0	2.0 (K10)
5	PN4	97.0	3.0 (K10)
6	PEN1	99.5	0.5 (Cloisite 30B)
7	PEN2	99.0	1.0 (Cloisite 30B)
8	PEN3	98.0	2.0 (Cloisite 30B)
9	PEN4	97.0	3.0 (Cloisite 30B)

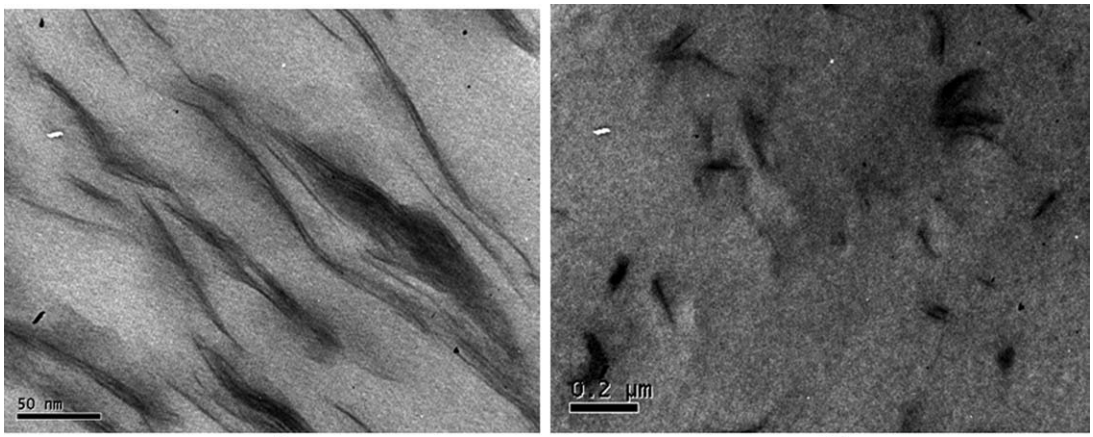

Figure 2 TEM micrographs of (a) PEN2; and (b) PEN4.

(Thru, Reflect, Line) calibration method using the calibration standards (Model: X11644A, Make: Agilent Technologies). The accuracy of waveguide setup was in the range of 1%. The verification of wave guide set up was carried out with known standard after the system calibration was completed to determine the measurement errors. However, no error was observed. Samples of PEI and PNC films of the size 22.86 × 10.16 mm were prepared for standard X band waveguide (WR90) sample holder. Micrometer (Least count 0.01 mm) was used for the measurement of thickness and the variation in thickness was observed in the range of ±0.01 mm. Measurement of thickness was carried out on various locations (minimum 5) of prepared sample to ensure the accuracy and uniformity of the thickness.

Loss tangent for all the samples was calculated from the ratio of measured values of imaginary part and real part of dielectric constant of the same sample.

Wide-angle X ray diffraction (WAXD) (Model: Rigaku Dmax 2500, Make: Rigaku Dmax, Japan) analysis was carried out on Cloisite 30B, K10, PEI film and PNC films. Transmission electron microscopy (TEM) (Model: Philips Tecnai F30, Make: M/s. FEI Company) was carried out on PEI/Cloisite 30B nanocomposites to examine the detailed morphology. The samples were sectioned to 50–70 nm with a diamond knife using microtome (Model: Leica Ultracut UCT Make: Leica, Vienna, Austria). The sections were collected on 300 mesh carbon coated copper grids from water boat and dried on filter paper. The scanning electron micrographs (SEM) (Model: Carl Zeiss EVO-50X VP, Low Vacuum SEM, Make: Carl Zeiss NTS GmbH, Germany) were taken for surfaces of PN samples to bring out the segregation and phase separation of K10.

RESULTS AND DISCUSSION

Morphology

WAXD

The 2θ value of Cloisite 30B and K10 were observed to be 5° and 5.7°, respectively.[5] The increase in the value of 2θ of Cloisite 30B (*d*-spacing: 18.1 Å) over K10 (*d*-spacing: 15.6 Å) was attributed to higher *d*-spacing.

Low intensity peaks were observed for PEN1, PEN2 and PEN3 for 2θ value between 3.7° and 4.4°. These peaks were attributed to the intercalation of Cloisite 30B and the reason for low intensity of these peaks was attributed to the partial exfoliation of Cloisite 30B.[5]

Partial intercalation was observed in PEN1, PEN2, and PEN3. No peak for intercalation was observed for PEN4 due to the formation of tactoids of reduced *d*-spacing caused by over packing of Cloisite 30B. Huang et al.[16] have reported that the increase in content of nanoclay causes reduction in swelling of intercalated layered silicate. No peak for intercalation was observed for PN samples, too. Shallow peaks were observed beyond 8° of 2θ value. This value of 2θ indicated that there was a reduction in the values of *d*-spacing. The reduction in the values of *d*-spacing led to the formation of immiscible tactoids which caused phase separation and agglomeration of nonreinforcing K10.

TEM

Exfoliation was dominant in PEN1 with a few intercalated sites. The dominance of exfoliation was attributed to the dispersion of Cloisite 30B platelets. Intercalation along with exfoliation was observed in

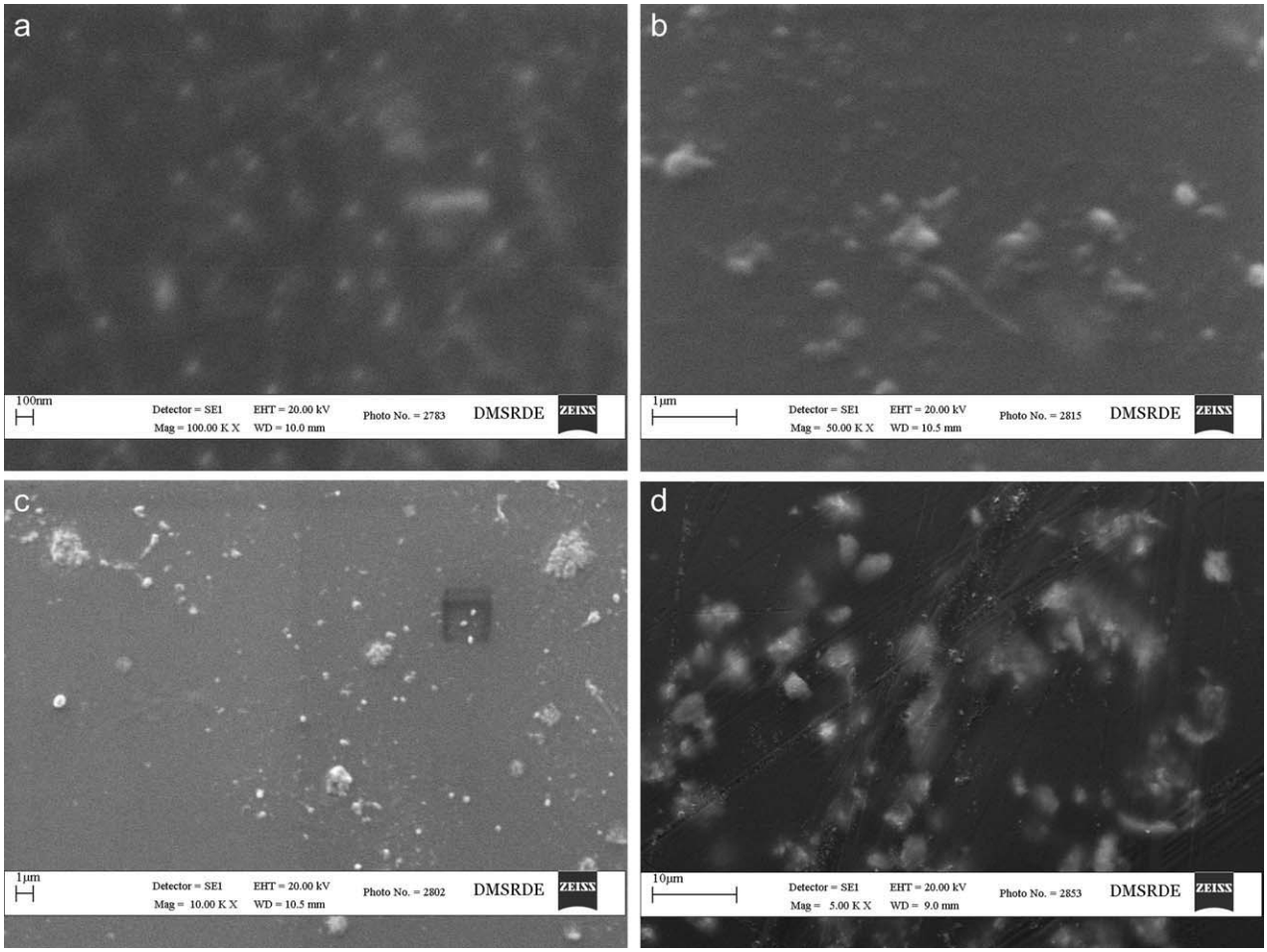

Figure 3 (a): SEM micrograph of PEN2. (b) SEM micrograph of PEN4. (c) SEM micrograph of PN2. (d) SEM micrograph of PN4.

PEN2. In PEN3, partial intercalation with a few sites of segregation indicated that at 2% weight content was more than optimum value. In PEN4, tactoids of Cloisite 30B were visible due to its segregation caused by super saturation by Cloisite 30B. The findings of TEM micrographs corroborated with the findings of the results of WAXD. Pozsgay et al. have reported that organophilization of nanoclay led to intercalation and exfoliation of nanoclay, but above particular weight % it behaved like particulate filler.[19] Typical TEM micrographs of PEN2 and PEN4 are shown in Figure 2(a,b), respectively.

There was no evidence of intercalation of K10 in PN samples in WAXD analysis, therefore, TEM was not carried out for the same.

SEM

The dispersion of Cloisite 30B was uniform in PEN1, PEN2, and PEN3, but phase separation and segregation were observed, in case of PEN4, from SEM micrographs. The dispersion of K10 was not uniform in PN samples, and phase separation and agglomeration were evident in PN samples. The results of SEM micrographs were in close compromise with the results of TEM for PEN samples. Typical SEM micrographs, depicting uniform dispersion in PEN2, and phase separation in PEN4, PN2, and PN4 are shown in Figure 3(a–d). The formation of tactoids of Cloisite 30B was quite visible in SEM micrograph of PEN4, as shown in Figure 3(b).

Dielectric behavior

Dielectric constant

The dielectric constant of K10 and Cloisite 30B was observed to be 2.5 and 1.7, respectively. The dielectric constant of PEI, PN, and PEN samples was observed 3.4, $\sim$ 4.0, and $\sim$ 3.7, respectively. The results of dielectric constant, loss tangent, transmission loss, and reflection loss are tabulated in Table II.

The role of microstructure and polarization in PNC is considered to be a complex phenomenon and has great influence on dielectric constant. In this

TABLE II
Values of Dielectric Constant, Loss Tangent, Transmission Loss, and Reflection Loss at X Band Frequency for PEI, PN, and PEN Samples

S. No.	Property	PEI	PN1	PN2	PN3	PN4	PEN1	PEN2	PEN3	PEN4
1.	Dielectric constant	3.4	3.8	3.8	3.8	4.0	3.7	3.7	3.7	3.8
2.	Loss tangent	0.05	0.05	0.04	0.06	0.03	0.03	0.03	0.02	0.02
3.	Transmission loss (dB)	−0.2	−0.4	−0.4	−0.2	−0.3	−0.2	−0.2	−0.2	−0.2
4.	Reflection loss (dB)	−0.5	−0.3	−0.4	−0.3	−0.4	−0.4	−0.3	−0.4	−0.3

study, the value of dielectric constant of PEI was observed to be marginally lower than that of PN and PEN. The reason for this might be attributed to hydrophobicity and reinforcing nature of Cloisite 30B which facilitated the dipole moment of long and rigid polymeric chain of PEI, in PEN samples. The interphase region between Cloisite 30B and PEI, in PEN samples, provided interconnectivity in PEI matrix. Thus, interfacial polarization and polarization of dipoles, in tiny and interconnected polymeric segments of PEI, caused an increase in dielectric constant over PEI. Whereas, in PN samples, K10 did not form any interphase with PEI because K10 was hydrophilic, and therefore, it caused plasticization of PEI. Plasticized PEI had non interconnected tiny segments of PEI. The presence of tiny plasticized PEI segments facilitated the dipole moment in PN samples to be better than that in PEN samples. Therefore, the values of dielectric constant of PN samples were higher than PEI and PEN samples.

Loss tangent

The loss tangent (tan δ) values of K10 and Cloisite 30B were calculated to be 0.2 and 0.1, respectively. The average values of tan δ for PEI, PN, and PEN were observed 0.05, 0.04, and 0.03, respectively. Values of tan δ of PEN samples were observed lower than that of PN samples due to better reinforcing nature of Cloisite 30B as discussed above. In PN samples, the values of loss tangent varied from 0.03 to 0.06. This was attributed to the inhomogeneous dispersion, of K10 as discussed earlier. The inhomogeneous mixing of K10 led to nonuniform distribution of dipoles/charges within PN samples. This phenomenon led to varied response of tan δ to EM wave. Whereas, a regular trend of tan δ was observed in PEN samples and this was attributed to the homogeneity of reinforcement in PEN samples.

Transmission loss

Transmission losses for PEN samples were comparatively lower than that for PN samples. The transmission losses for PEI, PN, and PEN samples were −0.2 dB, ∼ −0.3 dB, and −0.2 dB, respectively. The similarity in the values of transmission loss of PEN samples and PEI suggested that there was no adverse effect of Cloisite 30B on PEI in transmission loss. The transmission loss depend on dielectric constant, loss tangent, thickness of the dielectric material, internal reflection, refraction, Bore's sight error, side lobes, etc.[20,21] Varadan et al.[22] and Boughriet et al.[23] have reported that high values of loss tangent of materials have resulted in high transmission/reflection loss. The transmission loss for PN samples did not follow any trend, and values obtained were high as well as scattered due to the non reinforcing character of K10. The low values of tan δ of PEN samples had led to low values of transmission loss of PEN samples.

Reflection loss

EM wave transmitted, from a transmitter, was received back by a receiver through same dielectric material in the measurement of reflection loss. This phenomenon simulated the use of radome/nose cone in actual operation of aerospace vehicles. Also, internal reflections and refractions, of EM wave, occurred at each interface in the dielectric material when EM wave passed through it.[22,23] The values of reflection loss for PN and PEN samples were distributed in the range of −0.3 to −0.4 dB which were lower than the reflection loss of PEI which was measured −0.5 dB. The reason for this was same as explained above for transmission loss. The values of reflection loss might not follow any systematic trend with the values of transmission loss because in reflection loss an additional factor of interference of transmitting and reflecting EM wave played an important role apart from internal reflection, refraction, Bore's sight error, side lobes, etc.[20–22]

Tensile behavior

It was expected that the addition of nanoclay in the PEI matrix will change the mechanical properties of PNCs. The values of tensile strength, tensile modulus, and elongation at break for PEI, PN, and PEN samples are tabulated in Table III.

The values of tensile strength and elongation at break of PN samples were observed lower than that of PEI except the higher modulus value of PN1. This

TABLE III
Values of Tensile Strength, Tensile Modulus, and Elongation at Break of PEI, PN, and PEN Samples

S. No.	Sample name	Tensile strength (MPa)	Tensile modulus (MPa)	Elongation at break (%)
1	PEI	72.4	1309	6.6
2	PN1	72.7	1645	5.1
3	PN2	69.1	1750	4.8
4	PN3	59.3	1702	3.8
5	PN4	57.1	1612	4.0
6	PEN1	82.8	1753	5.5
7	PEN2	95.9	2236	5.0
8	PEN3	74.3	1887	4.5
9	PEN4	64.8	1655	4.4

was attributed to nonreinforcing nature of K10 and, rather, it behaved like particulate filler. K10, due to its non reinforcing nature, caused plasticization of PEI and led to discontinuity among polymeric chains of PEI. Segregation and phase separation of hydrophilic K10 in hydrophobic PEI was observed in SEM micrographs [refer Fig. 3(c,d)]. Therefore, increase in amount of K10, in PN samples, led to continuous lowering of tensile strength and strain, and increase in brittleness. The tensile strength of PN1 was found to be close to PEI due to limited filler effect of K10 at 0.5% of its content. The stress strain curves for PN samples are shown in Figure 4(a) and for PEI and PEN samples in Figure 4(b). Increase in modulus in PN samples was observed due to lowering of strain as shown in stress–strain curve.

Tensile strength and modulus of PEN samples were found be higher, by 10–25%, than that of PN samples for the similar content of nanoclay. Increase in tensile strength and modulus was observed due to reinforcing nature of Cloisite 30B. The reinforcing effect of Cloisite 30B was evident in PEN1 with higher values of tensile strength and modulus at 83 MPa and 1753 MPa, respectively, in comparison with the values of PN1 at 73 MPa and 1645 MPa, respectively. The increase in tensile strength was due to strong interfacial interaction between nanoclay and PEI. There was a formation of hydrogen bond between carbonyl group of PEI and hydroxyl group of Cloisite 30 B which has bis-2-hydroxy ethyl group. This hydrogen bond favored the stress transfer between PEI and Cloisite 30B. The maximum values of tensile strength, 95.9 MPa and modulus, 2236 MPa were observed for PEN2 and it implied that the optimum level of reinforcement with Cloisite 30B was 1% (by weight). These high values were also attributed to the presence of intercalation and exfoliation of Cloisite 30B in PEN samples. Intercalation and exfoliation, both, were important for the improvement of tensile properties of PNCs. Partial exfoliation provided the reinforcement of platelets at nanoscale level and caused interconnectivity among the polymeric chains of PEI in PNC. Intercalation caused local ordering of polymeric segment and also interconnectivity, with polymeric chains of PEI in the PNC. A reduction in tensile strength and modulus of PEN3 and PEN4 was observed due to segregation of Cloisite 30B. The brittleness of PEN samples was found to be lesser than that of PN samples due to better reinforcing nature of Cloisite 30B thereby making good interfacial bond with PEI. However, the brittleness kept on increasing with increasing content of Cloisite 30B because the strain kept on reducing as shown in stress strain curves for PEN samples in Figure 4(b). The reduction in strain was caused by segregation of Cloisite 30B, and at its high content, super saturation of Cloisite 30B occurred in PEI. The segregation caused resin starved areas which led to the discontinuity among polymeric chains of PEI matrix. Chen et al.[24] have found that the addition of 2% nanoclay and above in PEI has caused the brittleness in composites.

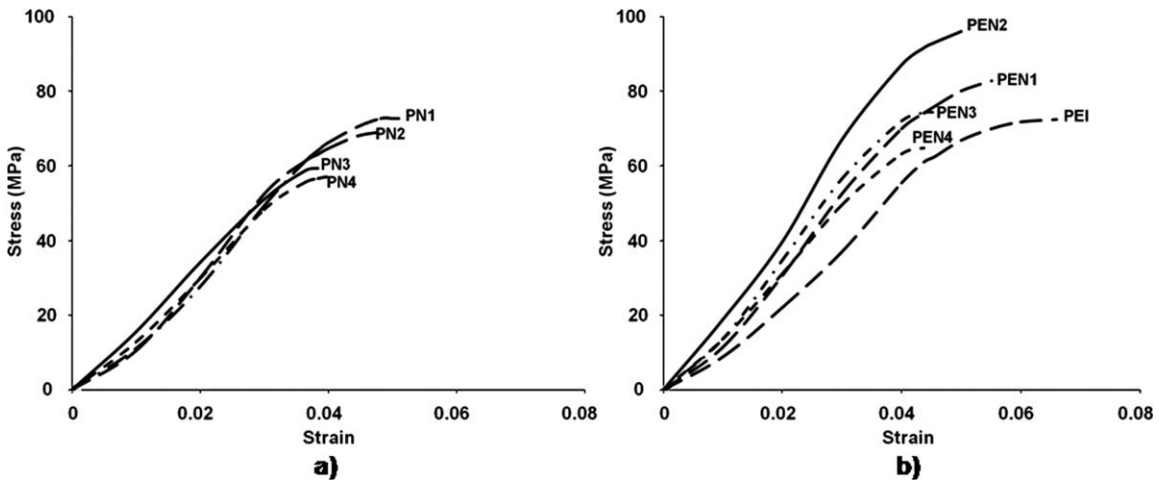

Figure 4 Stress–strain curves for (a) PN samples; and (b) PEI and PEN samples.

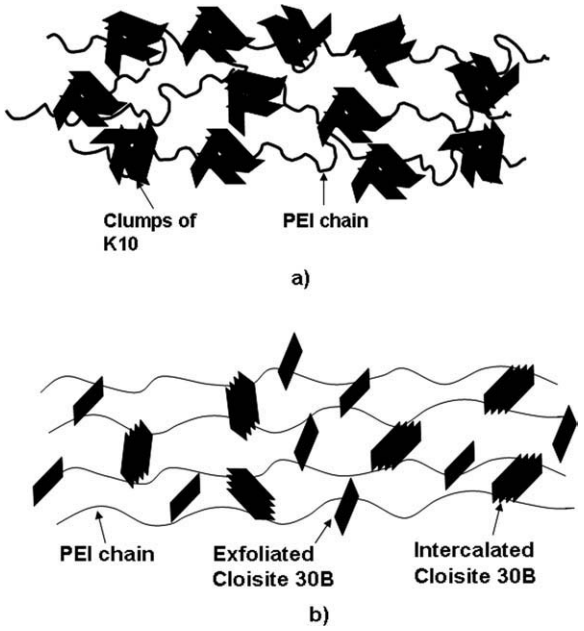

Figure 5 Schematic representation of (a) plasticization effect of K10; and (b) reinforcing effect of Cloisite 30B in PNCs.

Low strengths and strains with low elongation at break, of PN samples, were attributed to the phase separation and segregation of K10. It was evident from Figure 3(c) that the phase separation and phase segregation was dominant in PN samples. This effect led to the plasticization of PEI and, thus made it brittle. The clumps of K10, even after partial dispersion due to break down of clumps during sonication and casting, could not bind with the PEI matrix owing to their hydrophilic nature. They, rather, got agglomerated and caused plasticization effect. This effect in a form of schematic model has been shown in Figure 5(a). Whereas, in the case of PEN samples, segregation was evident only at 2% and above weight content of Cloisite 30B in PEI. The combination of intercalation and exfoliation of Cloisite 30B caused the connectivity among polymeric chains and was instrumental in load transfer when tensile forces were applied. This led to high strengths, strains, and elongation at break of PEN1 and PEN2 samples, with PEN2 having superior properties. The schematic model for this effect is shown in Figure 5(b).

CONCLUSIONS

The exfoliation and intercalation of nanoclay influence dielectric properties and tensile behavior of PEI/nanoclay composites. The values of dielectric constant, loss tangent, transmission/reflection losses were observed to be the minimum and tensile properties were observed to be the maximum for 1% reinforcement, by weight, of Cloisite 30B in PEI in the present study. Organoclay reinforced PEI nanocomposites were found to be the promising materials for the applications in EM transparent applications. Organoclay based PNC have a lot of scope for the future applications and will revolutionize the material research because they offer myriad of possibilities in the choice of materials and their processing.

The authors thank Dr. K.U.B. Rao, Director and Dr. R.K. Singh, Scientist of DMSRDE, Kanpur for their cooperation and support to complete this work.

References

1. Tsai, J.; Sun, C.T. J Comp Mater 2004, 38, 567.
2. Shabeer, A.; Chandrashekhara, K.; Schuman, T. J Comp Mater 2007, 41, 1825.
3. Tsay, S. Y.; Chen, B. K.; Chen, C.P. J Appl Polym Sci 2006, 99, 2966.
4. Dwivedi, M.; Alam, S.; Bhatnagar, N.; Ghosh, A. K. Polym Adv Technol, Published online on 30 July 2010. doi: 10.1002/pat.1740.
5. Dwivedi, M.; Alam, S.; Bhatnagar, N.; Ghosh, A. K. J Therm Compos Mater, Published online on 19 November 2010. doi: 10.1177/0892705710388745.
6. Zebouchi, N.; Truong, V. H.; ssolbi, R.; Se-Ondoua, M.; Malec, D.; Vella, N.; Malrieu, S.; Toureille, A.; Schue, F.; Jones, R. G. Polym Int 1999, 46, 54.
7. Chen, B.; Fang, Y.; Cheng, J. Macromol Sympos 2006, 242, 34.
8. Wang, H. W.; Chang K. C.; Yeh, J. M.; Liou, S. J. J Appl Polym Sci 2003, 91, 1368.
9. Wang, H. W.; Chang K. C.; Chu H. C.; Liou, S. J.; Yeh, J. M. J Appl Polym Sci 2004, 92, 2402.
10. Kashani M. R.; Gharavi, N.; Javadi, S. Smart Mater Struct 2008, 17, 065035.
11. Zhang, Y.; Dang, Z.; Fu, S.; Xin, S.; Deng, J.; Wu, J.; Yang, S.; Li, L.; Yan, Q. Chem Phys Lett 2005, 401, 553.
12. McBrearty, M.; Bur, A.; Roth, S. SPE ANTEC Conf Proc, 2000.
13. Dhibar, A. K.; Mallick, S.; Rath, T.; Khatua, B. B. J Appl Polym Sci 2009, 113, 3012.
14. Farzana, H.; Hojjati, M.; Okamoto, M.; Gorga R. E. J Comp Mater 2006, 40, 1511.
15. Maroulas, P.; Kripotou, S.; Pissis, P.; Fainleib, A.; Bei, I.; Bershtein, V.; Gomza, Y. J Comp Mater 2009, 43, 943.
16. Huang, R. Y. M.; Feng, X. J Appl Polym Sci 1995, 57, 613.
17. Morgan, A. B.; Gilman, J. W.; Jackson, C. L. Macromolecules 2001, 34, 2735.
18. Weiping, L.; Hoa, S.; Pugh, M. Compos Sci Technol 2005, 65, 2364.
19. Pozasgay, A.; Papp, L.; Frater, T.; Pukanszky, B. Polypropylene/Montmorillonite Nanocomposites Prepared by the Delamination of the Filler; Progress in Colloid and Polymer Science, Springer: Berlin/ Heidelberg, 2002.
20. Raghavan, V. Materials Science and Engineering; Prentice Hall of India Private Limited: New Delhi, 1989.
21. Kozakoff, D. J. Analysis of Radome-Enclosed Antennas; Artech House: Boston, 1997.
22. Varadan, V. V.; Hollinger, R. D.; Ghodgaonkar, D. K.; Varadan, V. K. IEEE Trans Microwave Theory Tech 1991, 40, 842.
23. Boughriet, A. H.; Legrand, C.; Chapoton, A. IEEE Trans Microwave Theory Tech 1997, 45, 52.
24. Chen, B. K.; Su, C. T.; Tseng, M. C.; Tsay, S. Y. Polym Bull 2006, 57, 671.